



HAL
open science

Ligand-induced twisting of nanoplatelets and their self-assembly into chiral ribbons

Santanu Jana, Marta de Frutos, Patrick Davidson, Benjamin Abécassis

► **To cite this version:**

Santanu Jana, Marta de Frutos, Patrick Davidson, Benjamin Abécassis. Ligand-induced twisting of nanoplatelets and their self-assembly into chiral ribbons. *Science Advances*, 2017, 3 (9), pp.e1701483. 10.1126/sciadv.1701483 . hal-01596102

HAL Id: hal-01596102

<https://hal.science/hal-01596102>

Submitted on 19 Nov 2020

HAL is a multi-disciplinary open access archive for the deposit and dissemination of scientific research documents, whether they are published or not. The documents may come from teaching and research institutions in France or abroad, or from public or private research centers.

L'archive ouverte pluridisciplinaire **HAL**, est destinée au dépôt et à la diffusion de documents scientifiques de niveau recherche, publiés ou non, émanant des établissements d'enseignement et de recherche français ou étrangers, des laboratoires publics ou privés.

NANOSTRUCTURES

Ligand-induced twisting of nanoplatelets and their self-assembly into chiral ribbons

Santanu Jana,^{1,2} Marta de Frutos,¹ Patrick Davidson,¹ Benjamin Abécassis^{1,2*}

The emergence of chirality is a central issue in chemistry, materials science, and biology. In nanoparticle assemblies, chirality has been shown to arise through a few different processes, but chiral organizations composed of plate-like nanoparticles, a class of material under scrutiny due to their wide applicative potential, have not yet been reported. We show that ribbons of stacked board-shaped cadmium selenide (CdSe) nanoplatelets (NPLs) twist upon the addition of oleic acid ligand, leading to chiral ribbons that reach several micrometers in length and display a well-defined pitch of ~400 nm. We demonstrate that the chirality originates from surface strain caused by the ligand because isolated NPLs in dilute solution undergo a transition from a flat to a twisted shape as the ligand coverage increases. When the platelets are closely stacked within ribbons, the individual twist propagates over the whole ribbon length. These results show that a ligand-induced mechanical stress can strongly distort thin NPLs and that this stress can be expressed at a larger scale, paving the way to stress engineering in assemblies of nanocrystals. Such a structural change resulting from a simple external stimulus could have broad implications for the design of sensors and other responsive materials.

INTRODUCTION

Assembling colloidal nanocrystals into structures of higher order is an important condition to exploit their electronic, photonic, or magnetic properties in devices (1). Among the variety of these superstructures, chiral arrangements are particularly desirable because they could bring up specific chiral properties beneficial for applications such as chiral catalysis, enantiospecific separation, or optical metamaterials (2). Chiral assemblies of nanoparticles have been shown to arise through a few different processes. The most common pathway is the use of a chiral template or ligand, which guides the assembly (3–5). For example, gold nanoparticles covered with purposely designed DNA ligands have been shown to arrange into chiral nanostructures, which display circular dichroism properties. When chiral ligands are attached at the surface of nanoparticles, they can break the symmetry of an achiral nanoparticle and act as a linking agent to induce nanoparticle chiral arrangements. However, other pathways have also been recently demonstrated. Photochemical reactions within CdS building blocks induce strain within ribbons of CdS/CdTe nanoparticles, which drives their twisting with a pitch of a few hundreds of nanometers (6). In another recent report, a magnetic field induces dipole-dipole interactions, which couple to other colloidal forces to induce the formation of chiral helices made of cubic magnetic nanoparticles (7).

Cadmium chalcogenide nanoplatelets (NPLs) are two-dimensional (2D) atomically flat nanoparticles coated with a monolayer of oleic acid (OA) ligand (8, 9). They display outstanding optical properties due to the extreme quantum confinement occurring along their thickness, such as pure fluorescent emission in the visible range, giant oscillator strength, low lasing threshold, or ultrafast fluorescence resonance energy transfer, which could all be exploited in future optoelectronic applications (10–15). Assembling these nanoparticles into larger superstructures paves the way toward tuning their excitonic properties in a controlled fashion (16), and assemblies such as giant anisotropic needles or threads composed of stacked NPLs that share similarities with living polymers have recently been obtained (17, 18).

Usual strategies to achieve nanocrystal self-assembly rely on tuning the repulsive and attractive interactions such as the short-range ligand repulsion or electrostatic interactions. For 2D nanoparticles (nanosheets and NPLs), compared to 1D nanoparticles (nanowires and nanorods), the influence of ligand-induced forces should be more important because the contact area between ligands is higher in the first case (19, 20). Previously reported mechanisms of controlled NPL self-assembly depend on the relative magnitude and range of these interactions, leading to tunable final structures (18, 21). These equilibrium approaches are based on the ability of the system to efficiently explore the configurational space and to choose the energetically favored configuration without getting trapped into secondary energy minima. However, this is most of the time not true, and nanoparticles, because of their intermediate size between those of molecules and colloids, often form out-of-equilibrium structures that persist over long times (22, 23). Our present strategy is to exploit the slow system dynamics to tune the shape of the nanoparticles during the self-assembly process. By doing so, we create new frustrated assemblies of colloidal NPLs. Frustration occurs whenever an incompatibility arises between short-range interactions dictating the positioning of particles and another geometrical constraint, like packing (24, 25). This antagonism can yield organizations that do not appear through classical self-assembly pathways. We applied this approach to NPLs that twist individually due to the mechanical stress caused by ligands covering their surface. However, when NPLs are already assembled face to face into stacks by evaporation, frustration arises from the particle close packing, which prevents the complete twisting of the NPL crystalline core, leading to the formation of chiral ribbons.

RESULTS

Five-monolayer (ML)-thick, board-shaped CdSe NPLs (8, 9) were synthesized as later described (see Materials and Methods). After thorough purification, the NPLs were dispersed in hexane. In their native state, they are covered with a monolayer of OA. Imaging by transmission electron microscopy (TEM) of a fresh dispersion shows that the NPLs have a flat board-like shape with mean edge lengths of 7 and 22 nm (Fig. 1, A to C), that is, with an in-plane aspect ratio of about 3.

¹Laboratoire de Physique des Solides, Université Paris-Saclay, CNRS, Université Paris-Sud, UMR 8502, 91405 Orsay, France. ²Laboratoire de Chimie, ENS de Lyon, CNRS, UMR 5182, Université Claude Bernard, Université de Lyon, 69007 Lyon, France.

*Corresponding author. Email: benjamin.abecassis@ens-lyon.fr

For NPL assembly, we use a drying scheme similar to that described in Jana *et al.* (18) (see Materials and Methods and Fig. 1D). However, instead of introducing a given amount of OA all at once before drying the colloidal dispersion, the total amount was divided in equal parts and added to the dispersion at regular intervals during drying. After drying, the precipitate was redispersed in hexane. TEM images of the resulting dispersion show ribbons (Fig. 2) composed of stacked NPLs, with a typical length ranging from 1 to 4 μm . Closer observation reveals that the ribbons are twisted. Instead of stacking face to face with parallel edges, consecutive NPLs in the same stack are rotated by a small angle, even though the NPLs remain centered on the ribbon axis. Therefore, an angular modulation appears along the ribbon with a period intermediate between the NPL thickness and the ribbon length. The distance over which particle rotation by 360° occurs (pitch) is typically around 400 nm. The pitch is uniform within each ribbon and over the different ribbons in the same sample. Electron tomography (Fig. 2I) on an individual ribbon reveals details of their 3D morphology, confirming their twisted nature. The presence of vacancy defects in the stacks, that is, places where one platelet seems to be missing, can also sometimes be noticed. Moreover, the shift between two neighboring platelets within a ribbon is not constant. In some parts, the platelets remain almost parallel, whereas fast platelet rotation occurs in other parts. We interpret these defects as drying artifacts because of the presence of the carbon film of the TEM grid. As the solvent evaporates, it is likely that hydrodynamic forces and particle adsorption sometimes distort the uniform helical structure of the threads to yield untwisted and twisted regions. These defects resemble 1D twist solitons (26, 27), which have already been observed in a variety of macromolecules.

As already observed in nontwisted threads of stacked square NPLs (18), the overall amount of OA in the medium affects the average length of the ribbons. In Fig. 2, TEM micrographs of twisted ribbons with two different OA concentrations are shown. For an OA total volume of 18 μl , added in three times to 6 ml of dispersion, small twisted stacks with a length below 1 μm are observed (Fig. 2D), whereas long

ribbons of several micrometers appear with a larger amount of OA (45 μl), added in the same way (Fig. 2, A to C).

From the electron tomography of 18 different ribbons, we observed that there are about equal numbers (10 versus 8) of clockwise and counterclockwise twisted ribbons. Moreover, the chirality of each ribbon remains the same over its whole length. Circular dichroism spectra of dispersions of twisted ribbons did not show any signal in the NPL absorption region, confirming the racemic nature of these dispersions. The fact that equal amounts of the two enantiomers are present in suspension suggests a stochastic process where a local fluctuation in a given ribbon randomly initiates twisting with one handedness. Once the handedness is selected, the twist propagates over the whole length of the ribbon.

To better understand the formation mechanism of the twisted ribbons, we investigated by TEM and small-angle x-ray scattering (SAXS) their intermediate formation stages by sampling small volumes of the drying suspension at different times (figs. S1 and S2). After the first addition of OA (step 1) and 1 day of drying, ribbons are already present in the solution, but they are not yet twisted. In contrast, after the second OA addition (step 2), some ribbons are twisted, but they do not display a regular pitch like in the final state (step 3). Instead, the pitch varies strongly within a given ribbon, and some ribbons are still not twisted. This suggests that twisting starts at random locations in some ribbons and that the pitch becomes uniform afterward, during drying. All SAXS patterns of the dispersion, at these three different steps (fig. S2), display two scattering peaks whose positions do not change over the whole process, confirming that the NPLs remain stacked and that the stacking period keeps constant. These results suggest that the combined effects of OA addition and evaporation make the NPL ribbons twist.

Infrared (IR) spectroscopy was used to investigate the organization of the alkane chains of the ligands coating the NPL during twisted ribbon self-assembly. Vibration bands in the CH_2 stretching region (2750 to 3000 cm^{-1}) provide information on the conformation of long

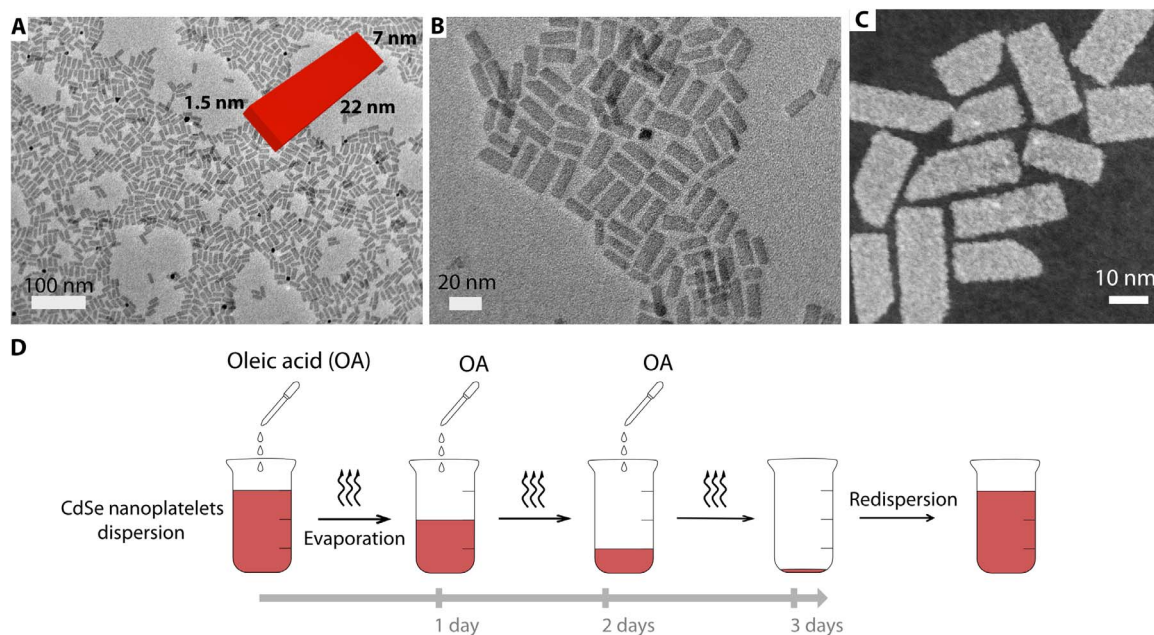


Fig. 1. NPL TEM characterization and drying assembly scheme. TEM (A and B) and STEM (C) images of the CdSe NPLs in their native form after synthesis and purification. They are 1.5 nm thick, 7 nm wide, and 22 nm long [inset of (A)]. (D) Scheme of the evaporation protocol used to obtain twisted ribbons.

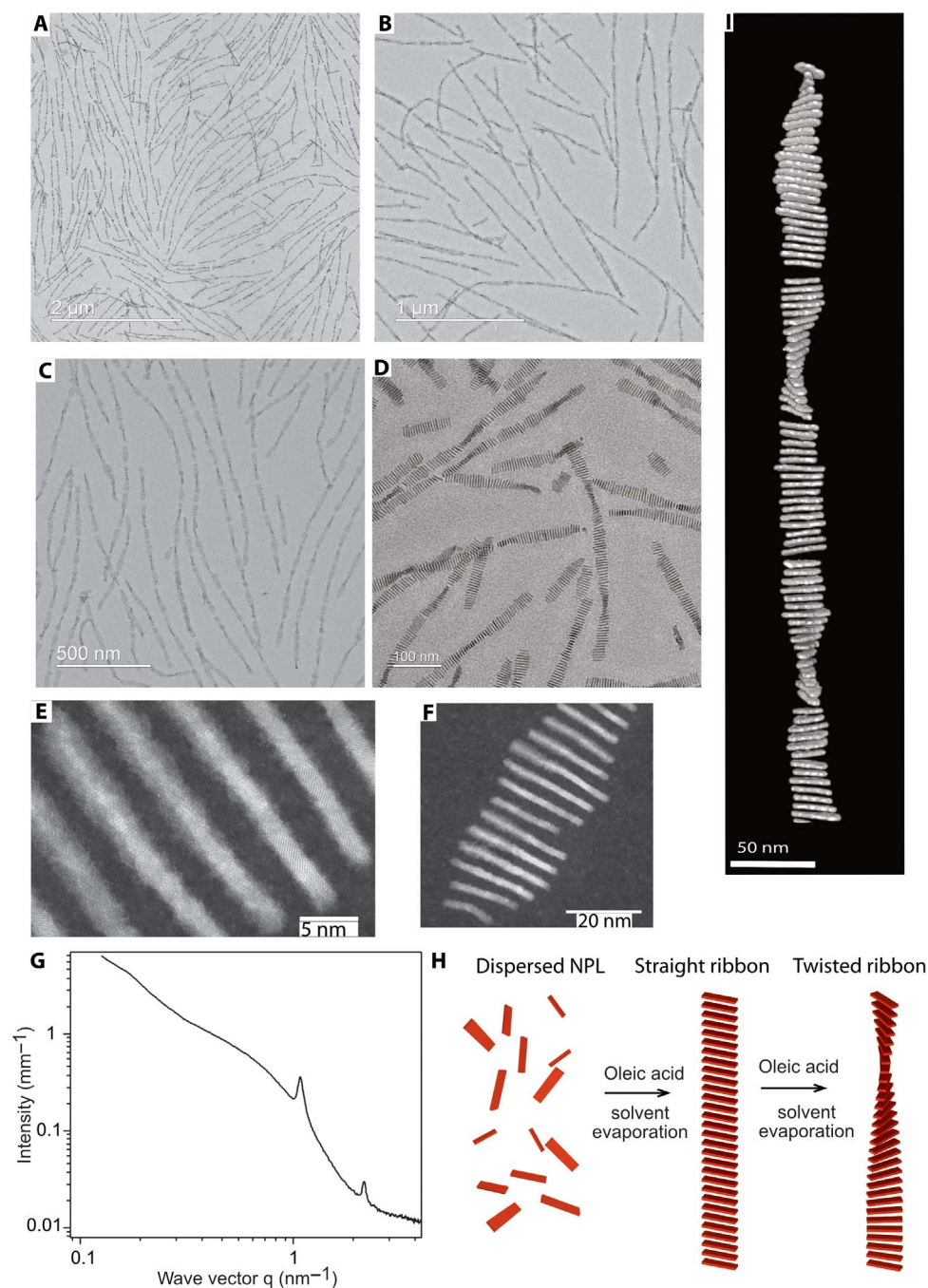


Fig. 2. Structural analysis of the twisted ribbons. (A to D) TEM images of twisted ribbons of various lengths at different magnifications. (E and F) HAADF-STEM images of twisted ribbons. The twist of the individual NPLs is small. (G) SAXS pattern of a dispersion of twisted ribbons. The two scattering peaks, at 1.0075 and 2.0141 nm^{-1} , respectively, are the first and second orders of diffraction from the NPL stacking and give the stacking period $d = 5.84$ nm. From this period, we deduce that there are around 70 NPLs within one pitch and that the mean rotation angle between two adjacent NPL is 5° . (H) Scheme of the twisted ribbon formation mechanism. Initially, flat NPLs are dispersed in solution. A first addition of OA followed by drying induces the formation of straight ribbons, which twist upon further addition of OA and drying. (I) 3D model from the tomographic reconstruction of a twisted ribbon.

aliphatic chains in the liquid or crystalline states. The IR spectra (fig. S3 and table S1) show that the d^+ symmetric methylene C–H stretching mode shifts from 2865 cm^{-1} for dispersed NPL to 2859 cm^{-1} for twisted ribbons. The intensity of the band is also much higher for the latter. A similar, albeit smaller, shift toward lower wave numbers is also observed for the d^- antisymmetric stretching mode. These facts

point to an increasing order of the alkyl chain brush as the self-assembly proceeds because the wave numbers of the d^+ and d^- transitions usually decrease upon liquid to crystalline transitions (28–31). Hence, the alkyl chains adopt a more ordered state, with more frequent all-trans conformations, during the formation of the twisted ribbons. This ordering of the ligands upon increase of surface coverage was recently demonstrated

in computer simulations of CdS quantum rods (32, 33). Because NPL purification is performed using ethanol, which is known to strip ligands off the particle surface (34), at the onset of self-assembly, the ligand brush should be sparse, with disorganized ligands having no preferential orientation. Upon OA addition, the surface coverage increases; this induces a higher degree of order of the alkyl chains, which, in turn, brings about the twisting of the ribbons through stress release.

To further test this scenario and confirm the presence of interfacial stress due to ligand adsorption, we added various amounts of OA to a dispersion of NPL in hexane without drying, to avoid ribbon formation. Then, the NPLs are not stacked and can freely change their shape upon ligand addition. The increase of OA concentration induced a transition of the individual NPL from a flat to a curved shape. When no OA is added, only flat NPLs are visible on the TEM grid (Figs. 1, A to C, and 3A). As the amount of OA increases, curved NPLs appear, and their proportion rises to almost 100% for $\sim 10 \mu\text{l}$ of OA added to 2 ml of NPL solution in hexane (Fig. 3, B, C, and G). High-angle annular dark-field (HAADF)-scanning TEM (STEM) (Fig. 3, D to F) images of the curved NPL display particles twisted like propeller blades, presenting a twist angle of $\sim 45^\circ$ occurring along their long edge. This

geometry was confirmed by electron tomography experiments (fig. S4). To determine the crystallographic direction of the twist, we indexed the reticular planes in the different areas of the twisted NPLs (figs. S5 and S6). The NPL's normal is along the [001] axis, whereas the long and short edges are along the [100] and [010] axes, respectively. Hence, the distorted geometry is obtained by twisting the initially flat NPLs along the [100] direction.

DISCUSSION

We now discuss the physical mechanism underlying this shape transition. Particle twisting usually involves negative Gaussian curvature and, therefore, stretching of the crystalline lattice. Because particle twisting is triggered by OA addition, the particle strain must be caused by ligand adsorption at the surface of the nanocrystals. Ligand self-assembly on surfaces can induce stress due to a mismatch between the crystalline and ligand lattices (35). Moreover, shifts of the IR vibration bands were also observed upon NPL twisting (fig. S7 and table S2). For plates, this elastic strain at the surfaces can induce twist (36–39) if the related energy is lower than that released by the surface organization of the ligands.

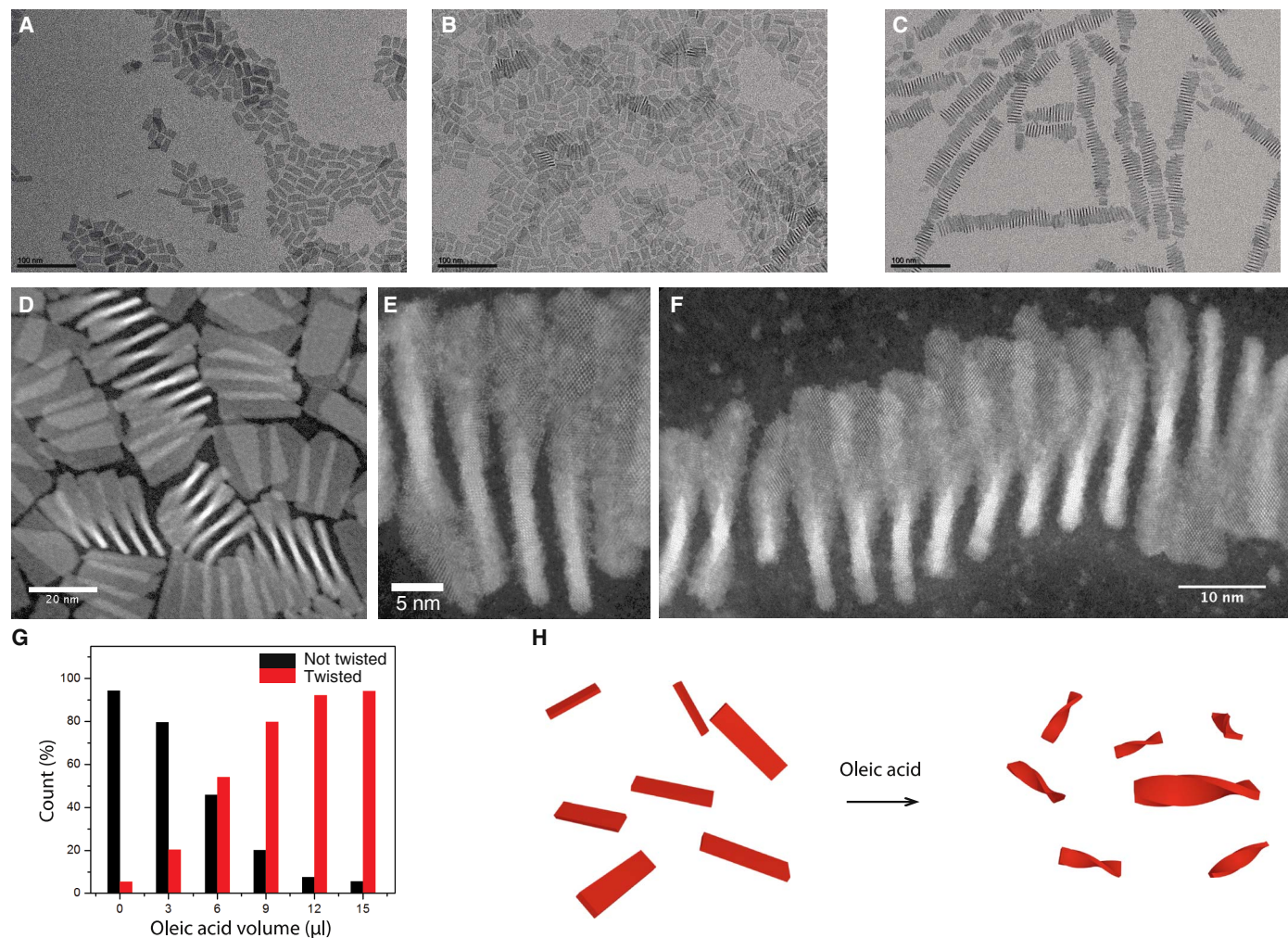


Fig. 3. Twisting of individual NPLs. (A to C) Electron microscopy of NPLs dispersed in solution upon increasing concentration of OA. In the absence of added OA (A), the NPLs are flat; the proportion of twisted NPL increases with the amount of added OA (B and C). (D to F) HAADF-STEM images of twisted NPLs. (G) Statistics of twisted and flat platelets counted on the TEM grid as a function of the quantity of OA added. (H) Scheme of the initially flat NPL twisting under the effect of the addition of OA.

The order of magnitude of the energy to twist by an angle θ a plate with shear modulus G , thickness e , and lateral dimensions w and L (with $L > w$) is, neglecting nonlinear terms (40): $E_t = \frac{2}{9} \frac{Gwe^3\theta^2}{L}$; with a shear modulus of 17.25 GPa (41), this corresponds to 12.5 eV per NPL. The ordering energy of a long-chain alkane ligand is typically 90 meV, as recently calculated by molecular dynamics (32). Hence, the ordering of only 140 ligands per NPL is required to match the twist energy. This represents a density of ~ 1 ligand/nm², which agrees well with the typical densities of ligands on semiconductor surfaces (0.6 to 4.6 ligands/nm²). Moreover, the helicoidal shape of the NPL involves negative Gaussian curvature, which is related to the presence of elastic strain (36).

Close inspection of the HAADF-STEM images of the chiral ribbons (Fig. 2F) reveals that within the assemblies, many of the NPLs are also twisted. However, the twist angle of the stacked NPL is only $\sim 10^\circ$, that is, much smaller than that observed ($\sim 45^\circ$) for isolated NPL. This could be due to van der Waals attractions between particles, which should flatten them to improve their packing. That is, the stacking constraint prevents the NPL from reaching their optimum twist deformation, leading to frustrated structures.

Although our experimental findings point to a change of surface stress induced by partial ligand adsorption and ordering, it is not clear yet how precisely OA is organized on the surface of the NPL. The flat-to-saddle-like shape transition suggests that there exists a gradient of strain between the center and the edges of the NPL. Compared to the original surface state, either the center is compressed and the edges are stress-free or the edges are dilated and the center remains unstrained. We expect partial crystallization to occur more favorably at the center of the plate because the ligands can explore more numerous configurations when they are located close to the edge. Under this hypothesis, increased packing order at the center of the NPL yields compressive stress on both sides of the NPL, and this stress decreases toward the particle rim. However, further experiments are needed to confirm this mechanism.

Here, we have shown that chiral ribbons made of CdSe NPLs could be formed through controlled drying of a colloidal dispersion while small amounts of OA ligand are added regularly. The physical origin of the twist lies in the strain induced by the ligands at the surface of the NPL. As the surface concentration increases, the conformation of the ligand alkyl chains changes and a gradient in ligand concentration is likely to build up on the faces of the NPLs. The configurational entropy of a ligand chain depends on its location on the faces of the NPLs because ligands close to the rim have more space to splay, whereas ligands in the center are more confined by a higher density of neighbors. We expect this inhomogeneity to play a role in the twisting at the NPL level. Thus, our work illustrates the potential of exploiting ligand-induced strain to tune the shape of 2D particles with thicknesses in the nanometer range. Together with out-of-equilibrium self-assembly strategies, this shape engineering method paves the way toward a better control of the orientational order within assemblies of nanocrystals. We expect that our approach should be easily generalized to other types of 2D nanoparticles and could be used to produce other original self-assembled nanostructures by tuning the internal strain transmitted by the ligands.

MATERIALS AND METHODS

NPL synthesis

Cadmium oleate (404 mg), selenium powder (27 mg) (100 mesh, Aldrich), and octadecene (25 ml) (90% Aldrich) were introduced into a 50-ml three-neck round bottom flask, equipped with a septum, a temperature

controller, and a condenser, and were kept under vacuum for 30 min. Afterward, the flask was purged with argon and the temperature was set to 240°C. At 180° to 190°C, the selenium started to dissolve and the solution turned clear yellow. When the temperature reached 205°C, the septum was withdrawn and 140 mg of cadmium acetate [Cd(OAc)₂, 2H₂O, Aldrich] was swiftly added into the flask. After the temperature reached 240°C, the reaction continued for 12 min, and 1 ml of OA was injected at the end. The flask was immediately cooled down to room temperature. At this stage, the reaction product was a mixture of 5-ML NPLs, a few 3-ML NPLs, and quantum dots in solution. The 5-ML NPLs were collected using size-selective precipitation by addition of ethanol and redispersion in hexane. This washing procedure was repeated three times, and NPLs were dispersed in hexane to prepare a stock solution for further self-assembly.

NPL ribbon twisting

One milliliter of the NPL stock solution was first diluted by adding 5 ml of hexane in a 20-ml vial to reach an optical density of the final NPL solution at 400 nm of 1.8. The dispersion was then sonicated for 10 min to obtain a clear transparent solution. The required amount of OA (for example, a total of 18 μ l to produce small ribbons) was used for the self-assembly experiment. For a typical example, OA was added in three steps during the slow drying process. The vial was kept with its cap slightly open at room temperature to slowly evaporate the solvent. Typically, 6 μ l of OA was initially added to the solution of NPL, mixed by gentle shaking, and then kept for slow drying by one-third of the total solution volume, which takes around 24 hours. At this time, 6 μ l of OA was added, and the drying process was resumed to evaporate two-thirds of the total solution volume within another 24 hours. Then, another 6 μ l of OA was added and the solution was completely dried in another 24 hours (total drying time of 72 hours). After complete evaporation, the deposit was redispersed in 4 ml of hexane. The dispersion looked slightly turbid and remained stable for days. To produce longer twisted ribbons, the procedure remains the same, but the volume of OA is increased from 18 to 45 μ l.

Electron microscopy

Samples were prepared by depositing a droplet of the suspension on commercial carbon TEM grids. They were first analyzed using an Akashi Topcon EM-002B for TEM imaging, and then, electron tomography measurements were carried out for representative samples. The tomographic tilt series were acquired using a JEM 2010 Field Emission Gun TEM (JEOL) operating at 200 kV, for tilt angles ranging from +60° to -60° with increments of 2°. Images were recorded on a Gatan Ultrascan 4K camera at a nominal defocus of -500 nm and a magnification of 50,000. Data were processed with IMOD software (42) for manual alignment and for reconstruction using the simultaneous iterative reconstructive technique (SIRT) method.

The atomic structure was analyzed by STEM on a Nion UltraSTEM 200 operating at 200 kV and an HAADF detector with an inner collection angle of 70 mrad. The microscope was equipped with a spherical aberration corrector.

Small-angle x-ray scattering

SAXS experiments were performed on the SWING beamline of the SOLEIL synchrotron, France (proposal number 20141010). Dispersions of self-assembled NPLs in hexane were transferred in glass capillaries. SAXS patterns were acquired, and images were reduced and normalized using standard beamline procedures.

SUPPLEMENTARY MATERIALS

Supplementary material for this article is available at <http://advances.sciencemag.org/cgi/content/full/3/9/e1701483/DC1>

- fig. S1. TEM images at different steps of the twisted threads formation.
 fig. S2. SAXS patterns at different steps of the twisted threads formation.
 fig. S3. Fourier transform IR (FTIR) spectra of NPL dispersions at different steps of the twisted thread formation.
 fig. S4. Electron tomography of individually twisted NPLs.
 fig. S5. High-resolution HAADF-STEM images of twisted NPLs.
 fig. S6. Crystallographic structure of CdSe NPLs.
 fig. S7. FTIR spectra of NPL dispersions in solution with varying amounts of OA without drying (that is, without assembly into threads).
 table S1. Position of the vibration bands for the symmetric and antisymmetric stretching bands corresponding to the spectra of fig. S3.
 table S2. Position of the vibration bands for the symmetric and antisymmetric stretching bands corresponding to the spectra of fig. S7.

REFERENCES AND NOTES

- M. A. Boles, D. V. Talapin, Self-assembly of tetrahedral CdSe nanocrystals: Effective "patchiness" via anisotropic steric interaction. *J. Am. Chem. Soc.* **136**, 5868–5871 (2014).
- W. Ma, L. Xu, A. F. de Moura, X. Wu, H. Kuang, C. Xu, N. A. Kotov, Chiral inorganic nanostructures. *Chem. Rev.* **117**, 8041–8093 (2017).
- J. Sharma, R. Chhabra, A. Cheng, J. Brownell, Y. Liu, H. Yan, Control of self-assembly of DNA tubules through integration of gold nanoparticles. *Science* **323**, 112–116 (2009).
- A. Kuzyk, R. Schreiber, Z. Fan, G. Pardatscher, E.-M. Roller, A. Högele, F. C. Simmel, A. O. Govorov, T. Liedl, DNA-based self-assembly of chiral plasmonic nanostructures with tailored optical response. *Nature* **483**, 311–314 (2012).
- C. Song, M. G. Blaber, G. Zhao, P. Zhang, H. C. Fry, G. C. Schatz, N. L. Rosi, Tailorable plasmonic circular dichroism properties of helical nanoparticle superstructures. *Nano Lett.* **13**, 3256–3261 (2013).
- S. Srivastava, A. Santos, K. Critchley, K.-S. Kim, P. Podsiadło, K. Sun, J. Lee, C. Xu, G. D. Lilly, S. C. Glotzer, N. A. Kotov, Light-controlled self-assembly of semiconductor nanoparticles into twisted ribbons. *Science* **327**, 1355–1359 (2010).
- G. Singh, H. Chan, A. Baskin, E. Gelman, N. Repnin, P. Král, R. Klajn, Self-assembly of magnetite nanocubes into helical superstructures. *Science* **345**, 1149–1153 (2014).
- S. Ithurria, B. Dubertret, Quasi 2D colloidal CdSe platelets with thicknesses controlled at the atomic level. *J. Am. Chem. Soc.* **130**, 16504–16505 (2008).
- S. Ithurria, M. D. Tessier, B. Mahler, R. P. S. M. Lobo, B. Dubertret, A. L. Efron, Colloidal nanoplatelets with two-dimensional electronic structure. *Nat. Mater.* **10**, 936–941 (2011).
- L. Biadala, F. Liu, M. D. Tessier, D. R. Yakovlev, B. Dubertret, M. Bayer, Recombination dynamics of band edge excitons in quasi-two-dimensional CdSe nanoplatelets. *Nano Lett.* **14**, 1134–1139 (2014).
- M. Peltón, S. Ithurria, R. D. Schaller, D. S. Dolzhenko, D. V. Talapin, Carrier cooling in colloidal quantum wells. *Nano Lett.* **12**, 6158–6163 (2012).
- C. E. Rowland, I. Fedin, H. Zhang, S. K. Gray, A. O. Govorov, D. V. Talapin, R. D. Schaller, Picosecond energy transfer and multiexciton transfer outpaces Auger recombination in binary CdSe nanoplatelet solids. *Nat. Mater.* **14**, 484–489 (2015).
- B. Guzelturk, M. Olutas, S. Delikanli, Y. Kelestemur, O. Erdem, H. V. Demir, Nonradiative energy transfer in colloidal CdSe nanoplatelet films. *Nanoscale* **7**, 2545–2551 (2015).
- B. Guzelturk, Y. Kelestemur, M. Olutas, S. Delikanli, H. V. Demir, Amplified spontaneous emission and lasing in colloidal nanoplatelets. *ACS Nano* **8**, 6599–6605 (2014).
- M. Olutas, B. Guzelturk, Y. Kelestemur, A. Yeltik, S. Delikanli, H. V. Demir, Lateral size-dependent spontaneous and stimulated emission properties in colloidal CdSe nanoplatelets. *ACS Nano* **9**, 5041–5050 (2015).
- B. Guzelturk, O. Erdem, M. Olutas, Y. Kelestemur, H. V. Demir, Stacking in colloidal nanoplatelets: Tuning excitonic properties. *ACS Nano* **8**, 12524–12533 (2014).
- B. Abécassis, M. D. Tessier, P. Davidson, B. Dubertret, Self-assembly of CdSe nanoplatelets into giant micrometer-scale needles emitting polarized light. *Nano Lett.* **14**, 710–715 (2014).
- S. Jana, P. Davidson, B. Abécassis, CdSe nanoplatelets: Living polymers. *Angew. Chem. Int. Ed.* **55**, 9371–9374 (2016).
- S. C. Glotzer, Nanotechnology: Shape matters. *Nature* **481**, 450–452 (2012).
- M. R. Jones, R. J. Macfarlane, A. E. Prigodich, P. C. Patel, C. A. Mirkin, Nanoparticle shape anisotropy dictates the collective behavior of surface-bound ligands. *J. Am. Chem. Soc.* **133**, 18865–18869 (2011).
- S. Jana, T. N. T. Phan, C. Bouet, M. D. Tessier, P. Davidson, B. Dubertret, B. Abécassis, Stacking and colloidal stability of CdSe nanoplatelets. *Langmuir* **31**, 10532–10539 (2015).
- Y. Min, M. Akbulut, K. Kristiansen, Y. Golan, J. Israelachvili, The role of interparticle and external forces in nanoparticle assembly. *Nat. Mater.* **7**, 527–538 (2008).
- S. Whitelam, R. L. Jack, The statistical mechanics of dynamic pathways to self-assembly. *Annu. Rev. Phys. Chem.* **66**, 143–163 (2015).
- G. M. Grason, Perspective: Geometrically frustrated assemblies. *J. Chem. Phys.* **145**, 110901 (2016).
- G. M. Grason, Colloquium: Geometry and optimal packing of twisted columns and filaments. *Rev. Mod. Phys.* **87**, 401–419 (2015).
- M. Mansfield, R. H. Boyd, Molecular motions, the α relaxation, and chain transport in polyethylene crystals. *J. Polym. Sci. Polym. Phys. Ed.* **16**, 1227–1252 (1978).
- J. L. Skinner, P. G. Wolynes, Solitons, defect diffusion, and dielectric relaxation of polymers. *J. Chem. Phys.* **73**, 4022–4025 (1980).
- R. G. Nuzzo, L. H. Dubois, D. L. Allara, Fundamental studies of microscopic wetting on organic surfaces. 1. Formation and structural characterization of a self-consistent series of polyfunctional organic monolayers. *J. Am. Chem. Soc.* **112**, 558–569 (1990).
- M. J. Hostetler, J. J. Stokes, R. W. Murray, Infrared spectroscopy of three-dimensional self-assembled monolayers: *N*-Alkanethiolate monolayers on gold cluster compounds. *Langmuir* **12**, 3604–3612 (1996).
- R. G. Snyder, H. L. Strauss, C. A. Elliger, Carbon-hydrogen stretching modes and the structure of *n*-alkyl chains. 1. Long, disordered chains. *J. Phys. Chem.* **86**, 5145–5150 (1982).
- R. A. MacPhail, H. L. Strauss, R. G. Snyder, C. A. Elliger, Carbon-hydrogen stretching modes and the structure of *n*-alkyl chains. 2. Long, all-trans chains. *J. Phys. Chem.* **88**, 334–341 (1984).
- A. Widmer-Cooper, P. Geissler, Orientational ordering of passivating ligands on CdS nanorods in solution generates strong rod-rod interactions. *Nano Lett.* **14**, 57–65 (2014).
- A. Widmer-Cooper, P. L. Geissler, Ligand-mediated interactions between nanoscale surfaces depend sensitively and nonlinearly on temperature, facet dimensions, and ligand coverage. *ACS Nano* **10**, 1877–1887 (2016).
- A. Hassinen, I. Moreels, K. De Nolf, P. F. Smet, J. C. Martins, Z. Hens, Short-chain alcohols strip X-type ligands and quench the luminescence of PbSe and CdSe quantum dots, acetonitrile does not. *J. Am. Chem. Soc.* **134**, 20705–20712 (2012).
- F. Bertolotti, D. N. Dirin, M. Ibáñez, F. Krumeich, A. Cervellino, R. Frison, O. Voznyy, E. H. Sargent, M. V. Kovalenko, A. Guagliardi, N. Masciocchi, Crystal symmetry breaking and vacancies in colloidal lead chalcogenide quantum dots. *Nat. Mater.* **15**, 987–994 (2016).
- R. Ghafouri, R. Bruinsma, Helicoid to spiral ribbon transition. *Phys. Rev. Lett.* **94**, 138101 (2005).
- S. Armon, E. Efrati, R. Kupferman, E. Sharon, Geometry and mechanics in the opening of chiral seed pods. *Science* **333**, 1726–1730 (2011).
- R. L. B. Selinger, J. V. Selinger, A. P. Malanoski, J. M. Schnur, Shape selection in chiral self-assembly. *Phys. Rev. Lett.* **93**, 158103 (2004).
- J. V. Selinger, M. S. Spector, J. M. Schnur, Theory of self-assembled tubules and helical ribbons. *J. Phys. Chem. B* **105**, 7157–7169 (2001).
- H. D. Keith, F. J. Padden Jr., Twisting orientation and the role of transient states in polymer crystallization. *Polymer* **25**, 28–42 (1984).
- R. W. Meulenber, T. Jennings, G. F. Strouse, Compressive and tensile stress in colloidal CdSe semiconductor quantum dots. *Phys. Rev. B* **70**, 235311 (2004).
- J. Kremer, D. Mastronarde, J. McIntosh, Computer visualization of three-dimensional image data using IMOD. *J. Struct. Biol.* **116**, 71–76 (1996).

Acknowledgments: We thank G. Grason, R. Kamien, R. Wensik, J.-F. Sadoc, and D. Constantin for discussions. This work has benefited from the platform and expertise of the Electron Microscopy Facility of the Institute for Integrative Biology of the Cell (I2BC). We are grateful to J. Perez for assistance during beamtime and to the SOLEIL staff for smoothly running the facility. **Funding:** This work was supported by "Investissements d'Avenir" LabEx PALM (ANR-10 LABX-0039-PALM). This project has received funding from the European Union's Horizon 2020 research and innovation program under the Marie Skłodowska-Curie grant (agreement no. 661199). The Nion UltraSTEM microscope is partially funded via the CNRS-Commissariat à l'Energie Atomique et aux Energies Alternatives "METSAs" French network (FR CNRS 3507) and the European Union grant no. 312483-ESTEEM2. **Author contributions:** B.A. conceived and directed the research. B.A. and P.D. supervised the project. S.J. discovered the phenomena and performed all the experiments except the high-resolution electron microscopy and tomography, which were performed by M.d.F. B.A. wrote the paper with edits from P.D. **Competing interests:** The authors declare that they have no competing interests. **Data and materials availability:** All data needed to evaluate the conclusions in the paper are present in the paper and/or the Supplementary Materials. Additional data related to this paper may be requested from B.A. (benjamin.abecassis@ens-lyon.fr).

Submitted 5 May 2017
 Accepted 26 July 2017
 Published 13 September 2017
 10.1126/sciadv.1701483

Citation: S. Jana, M. de Frutos, P. Davidson, B. Abécassis, Ligand-induced twisting of nanoplatelets and their self-assembly into chiral ribbons. *Sci. Adv.* **3**, e1701483 (2017).

Ligand-induced twisting of nanoplatelets and their self-assembly into chiral ribbons

Santanu Jana, Marta de Frutos, Patrick Davidson and Benjamin Abécassis

Sci Adv 3 (9), e1701483.

DOI: 10.1126/sciadv.1701483

ARTICLE TOOLS

<http://advances.sciencemag.org/content/3/9/e1701483>

SUPPLEMENTARY MATERIALS

<http://advances.sciencemag.org/content/suppl/2017/09/11/3.9.e1701483.DC1>

REFERENCES

This article cites 42 articles, 4 of which you can access for free
<http://advances.sciencemag.org/content/3/9/e1701483#BIBL>

PERMISSIONS

<http://www.sciencemag.org/help/reprints-and-permissions>

Use of this article is subject to the [Terms of Service](#)

Science Advances (ISSN 2375-2548) is published by the American Association for the Advancement of Science, 1200 New York Avenue NW, Washington, DC 20005. The title *Science Advances* is a registered trademark of AAAS.

Copyright © 2017 The Authors, some rights reserved; exclusive licensee American Association for the Advancement of Science. No claim to original U.S. Government Works. Distributed under a Creative Commons Attribution NonCommercial License 4.0 (CC BY-NC).